Chinese Chemical Letters 32 (2021) 918–922

Contents lists available at ScienceDirect

Chinese Chemical Letters

journal homepage: www.elsevier.com/locate/cclet

Communication

A stable Co(II)-based metal-organic framework with dual-functional pyrazolate-carboxylate ligand: Construction and CO_2 selective adsorption and fixation

Guangrui Si, Xiangjing Kong, Tao He, Wei Wu, Linhua Xie, Jianrong Li*

Beijing Key Laboratory for Green Catalysis and Separation and Department of Environmental Chemical Engineering, Beijing University of Technology, Beijing 100124, China

ARTICLE INFO

Article history:
Received 9 June 2020
Received in revised form 9 July 2020
Accepted 13 July 2020
Available online 15 July 2020

Keywords:
Metal-organic framework (MOF)
Pyrazolate-carboxylate ligand
Construction
CO_2 selective adsorption
CO_2 fixation

ABSTRACT

By taking the functional advantages of both pyrazolate and carboxylate ligands, a unique dual-functional pyrazolate-carboxylate ligand acid, 4-(3,6-di(pyrazol-4-yl)-9-carbazol-9-yl)benzoic acid (H_3PCBA) was designed and synthesized. Using it, a new Co(II)-based metal-organic framework (MOF), Co_3(PCBA)$_2$(H_2O)$_2$ (BUT-75) has been constructed. It revealed a (3,6)-connected net based on the 6-connected linear trinuclear metal node, and showed good chemical stability in a wide pH range from 3 to 12 at room temperature, as well as in boiling water. Due to the presence of rich exposed Co(II) sites in pores, BUT-75 presented high selective CO_2 adsorption capacity over N_2 at 298 K. Simultaneously, it demonstrated fine catalytic performance for the cycloaddition of CO_2 with epoxides into cyclic carbonates under ambient conditions. This work has not only enriched the MOF community through integrating diverse functionalities into one ligand but also contributed a versatile platform for CO_2 fixation, thereby pushing MOF chemistry forward by stability enhancement and application expansion.

Metal-organic frameworks (MOFs), as an emerging family of crystalline porous materials, have attracted extensive attention for their potential applications in various fields, such as gas storage and separation [1], proton conduction [2], biomedicine [3], chemical sensing [4], heterogeneous catalysis [5] and so forth. Owing to the modular nature of MOFs, their structure and function allow precise tunability by the programmed assembly of diverse organic linkers and inorganic nodes [6–8]. However, the issue of the unsatisfactory chemical stability of MOFs has limited their practical applications.

Based on Pearson's hard/soft acid/base (HSAB) principle [9], MOFs constructed either from high-valent metals (hard acids, including Zr^{4+}, Hf^{4+}, Fe^{3+}, Al^{3+}) and carboxylate ligands (hard bases) [10,11], or from low-valent metal ions (soft acids, including Zn^{2+}, Co^{2+}, Ni^{2+}) and azolate ligands (soft bases) [12,13], inherently show good chemical stability originated from the robust coordination bonding. Despite excellent acid stability, the carboxylate-based MOFs usually have poor durability under basic conditions; by contrast, the azolate-based analogues exhibiting high base resistance are inevitably vulnerable to acidic species [14,15]. It can be found that the nature of coordination bond has imposed great restriction on the stability of most MOFs [16–18]. Therefore, developing new MOFs stable in a large pH scope would advance the MOF community toward expansive applications.

The utilization of dual-functional azolate-carboxylate ligands offers a simple yet effective approach to construct stable MOFs superior to either their azolate- or carboxylate-based counterparts. In this regard, there are several dual-functional azolate-carboxylate ligands employed, showing different combinations of functional groups, size, and symmetry (Scheme 1) [19–23]. Among various azolate ligands, pyrazolates with the highest pKa value usually endow the resulting MOFs with enhanced stability by connecting low-valent metal ions. Furthermore, a multifunctional ligand containing more pyrazolate moieties tends to afford more stable MOFs. Therefore, we speculate that a dual-functional pyrazolate-carboxylate ligand bearing more pyrazolate groups would contribute to MOFs with better chemical stability. To date, dual-functional pyrazolate-carboxylate ligand-based MOFs are seldom reported mainly attributed to synthetic difficulties of these ligands and MOF crystals. In addition, the simultaneous coordination of pyrazolate and carboxylate groups with metal centers would afford novel architectures showing high robustness and diverse functionality, which attracts our interest in further exploration.

* Corresponding author.
E-mail address: jrli@bjut.edu.cn (J. Li).

https://doi.org/10.1016/j.cclet.2020.07.023
1001-8417/

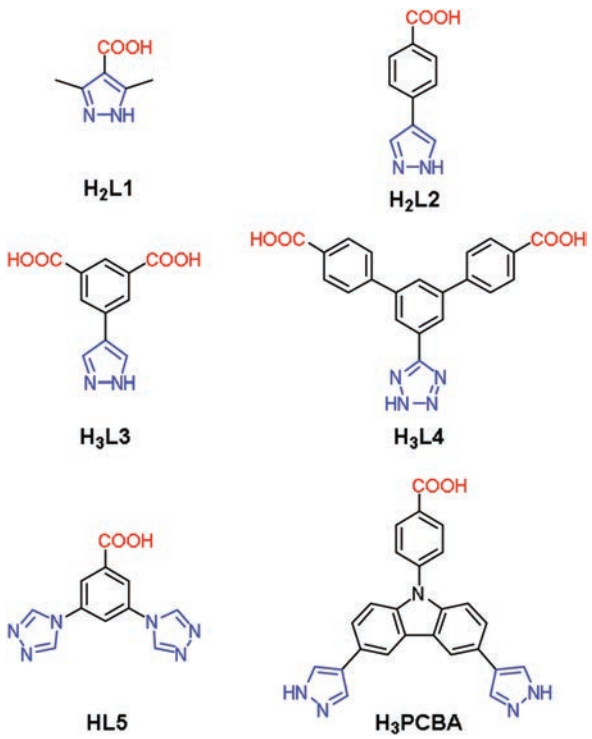

Scheme 1. Dual-functional azolate-carboxylate ligand acids reported in the literatures and H_3PCBA used in this work.

Herein, we report a stable Co(II)-MOF, $Co_3(PCBA)_2(H_2O)_2$ (BUT-75, BUT = Beijing University of Technology) constructed from a unique dual-functional pyrazolate-carboxylate ligand $PCBA^{3-}$ with low symmetry ($PCBA^{3-}$ = 4-(3,6-di (1*H*-pyrazolate-4-yl)-9*H*-carbazol-9-yl))benzoate). By integrating the advantages of both pyrazolate and carboxylate ligands for constructing stable MOFs, BUT-75 with linear 6-connected Co_3 clusters thus showed good chemical stability in aqueous solutions of a wide pH range (3-12) and boiling water. With abundant open Co(II) sites in the framework, this MOF also presented high CO_2 affinity and thus high selective CO_2 adsorption capacity over N_2 at 298 K. In addition, BUT-75 demonstrated high catalytic activity toward the CO_2-epoxide cycloaddition reaction under ambient conditions. This work offers a typical example of building stable versatile MOFs from dual-functional ligands, meanwhile contributes an effective adsorbent for selective CO_2 capture, as well as a recyclable heterogeneous catalyst for CO_2 conversion.

The solvothermal reaction between H_3PCBA and Co $(OAc)_2{\cdot}4H_2O$ in 2 mL of *N*,*N*-dimethylformamide (DMF), 0.2 mL of water and 80 μL of triethylamine at 120 °C for 48 h afforded hexagonal dark purple crystals of BUT-75, $Co_3(PCBA)_2(H_2O)_2$ (Fig. S2 in Supporting information). Single-crystal X-ray diffraction (SXRD) analysis revealed that BUT-75 crystallizes in the cubic crystal system with the $I2_13$ (No. 199) space group. The asymmetric unit of BUT-75 contains two kinds of crystallographically independent cobalt atoms (Co1 and Co2), one $PCBA^{3-}$ ligand and one H_2O molecule (Fig. 1a). Co1 (1/2 site occupancy) coordinates with four N atoms of the pyrazolate moieties from four different $PCBA^{3-}$ ligands in the tetrahedron coordination geometry. Co2 connects to two N atoms of pyrazolates from two different ligands, one O atom from the monodentate carboxylate of another ligand and one O atom of the terminal H_2O, showing a distorted tetrahedron geometry. One central Co1 and two lateral Co2 atoms are bridged together by four pyrazolates to form a linear Co_3 cluster (Fig. 1b) [24,25]. Each Co_3 cluster links six $PCBA^{3-}$ ligands through four pyrazolates and two carboxylates, as well as two terminal H_2O molecules; each $PCBA^{3-}$ ligand bridges three Co_3 clusters to afford the final three-dimensional (3D) structure of BUT-75. Topologically, the $PCBA^{3-}$ ligand and Co_3 cluster node can be simplified as a 3- and 6-connected node, respectively. The 3D framework of BUT-75 can thus be seen as a (3,6)-connected net with the point symbol of $(6^3)_2(6^7.8^8)$, as calculated by Topos (Fig. S3 in Supporting information). BUT-75 has a novel framework structure, where a rhombic channel (accommodating a cylinder with a diameter of 8.4 Å) and a triangular channel (accommodating a cylinder with a diameter of 9.7 Å) are observed (Figs. 1c and d). The solvent-accessible volume of BUT-75 is estimated to be 56% after the removal of free solvent molecules by PLATON [26].

In the structure, the $PCBA^{3-}$ ligand shows some configuration distortion by rotating the peripheral aromatic rings away from the central carbazole plane. The dihedral angle between the phenyl and carbazole ring is 56.79°, and that between pyrazolate containing the N1/N3 atom and the carbazole plane is 9.13°/18.29°, respectively, thus well matching the coordination geometry of the formed linear Co_3 cluster in BUT-75. It is worth noting that terminal H_2O molecules coordinated to the Co_3 cluster would afford open metal sites in BUT-75 after being removed.

To check the phase purity and crystallinity, the obtained BUT-75 sample was characterized by powder X-ray diffraction (PXRD). As shown in Fig. 2a and Fig. S7 (Supporting information), the diffraction pattern of the as-synthesized sample is in agreement with the simulated pattern from the crystal structural data, demonstrating high phase purity of this MOF. To investigate the coordination between ligands to metals in BUT-75, the FT-IR spectrum of the activated MOF sample was recorded in comparison with the ligand H_3PCBA. As shown in Fig. S4 (Supporting information), the characteristic peaks for stretching vibration of C=O bond in carboxyl groups and C=N bond in pyrazolyl groups at near 1720 cm^{-1} and 1601 cm^{-1} were found in the spectrum of H_3PCBA, however, their corresponding peaks were observed at 1599 cm^{-1} and 1481 cm^{-1} in BUT-75, respectively. The redshifts could be attributed to the coordination of carboxylates and pyrazolates to metal ions. The permanent porosity of BUT-75 was then examined by N_2 adsorption at 77 K. As shown in Fig. 2b, the

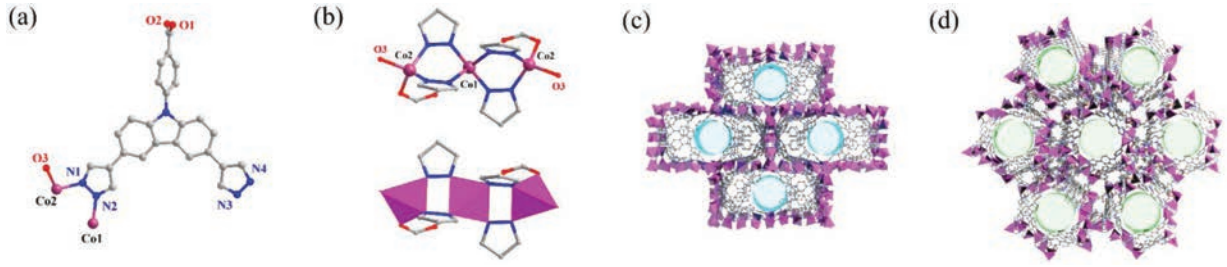

Fig. 1. (a) Asymmetric unit of BUT-75 structure. (b) Structure of the linear 6-connected Co_3 cluster in BUT-75. 3D network of BUT-75 showing 1D (c) rhombic and (d) triangular channels. H atoms are omitted for clarity.

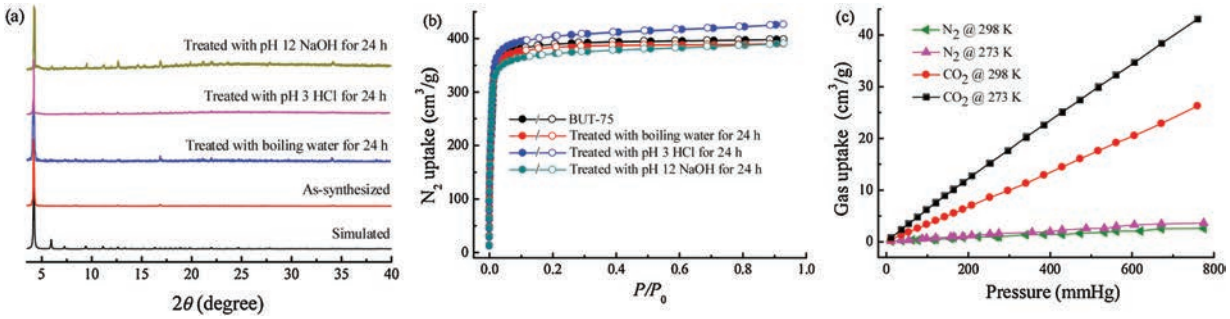

Fig. 2. (a) PXRD patterns simulated from the BUT-75 structure and of samples after different treatments. (b) N_2 adsorption/desorption isotherms of BUT-75 sample and of those after different treatments at 77 K. (c) CO_2 and N_2 adsorption isotherms for BUT-75 at 273 K and 298 K.

Type-I N_2 adsorption/desorption isotherms show a saturated N_2 uptake of 398 cm^3/g in the microporous BUT-75, and the evaluated Brunauer-Emmett-Teller surface area is 1498 m^2/g. Based on the N_2 adsorption data, the pore size distribution of BUT-75 is in the range from 5 Å to 10 Å as calculated by the density functional theory (DFT) method (Fig. S5 in Supporting information), being consistent with the result of crystallographic structure analysis. These results have further confirmed the structure of BUT-75, encouraging us to explore its properties.

The good stability of a new MOF material is necessary for its involvement in various applications. The stability of BUT-75 has thus been investigated. As can be seen from the thermogravimetric curve (Fig. S6 in Supporting information), BUT-75 can be thermally stable up to 420 °C, proving fine thermal stability. To confirm the chemical robustness of BUT-75, the samples were soaked in HCl aqueous solution (pH 3), NaOH aqueous solution (pH 12) at room temperature, and in boiling water for 24 h, respectively. As expected, the PXRD patterns of these treated samples remain almost unchanged compared with the as-synthesized sample, demonstrating no phase transition or framework collapse in tests (Fig. 2a and Fig. S7 in Supporting information) [27]. It can also be seen that peak intensities of high 2θ Bragg angles are relatively weak, which is mainly caused by the higher peak intensity ratios of peaks located at around 4.2° compared to those of high angles. In addition, the N_2 sorption isotherms of the treated samples are nearly identical to that of the untreated sample, further indicating the high chemical stability of BUT-75 (Fig. 2b). The strong acidic/basic resistance of BUT-75 may be mainly attributed to the use of the dual-functional H_3PCBA ligand, in which the co-existence of pyrazolate and carboxylate moieties enhances the stability of the resulting MOF. Such stability lays the foundation for BUT-75 to be exploited in significant applications.

With rich open Co(II) sites and good chemical stability, BUT-75 may be an excellent sorbent candidate for gas adsorption. Therefore, the gas adsorption measurements of pure CO_2 and N_2 over BUT-75 were experimentally conducted at 298 K and 273 K, respectively, and the results are shown in Fig. 2c. The maximum uptakes of CO_2 and N_2 are 43.1 and 3.6 cm^3/g at 273 K, and 26.3 and 2.6 cm^3/g at 298 K. It can be found that the uptakes of CO_2 are significantly higher than those of N_2, showing the potential of BUT-75 in selective CO_2 adsorption over N_2 [28]. In order to evaluate the adsorption selectivities of BUT-75 for CO_2/N_2, the initial slopes of their adsorption isotherms were fitted at low-pressure ranges as reported [29]. The estimated CO_2/N_2 selectivities are 10.0:1.0 at 273 K and 8.0:1.0 at 298 K (Fig. S8 in Supporting information), suggesting that BUT-75 could selectively adsorb CO_2 over N_2. Based on the CO_2 adsorption data, the CO_2 sorption heat (Q_{st}) of BUT-75 is calculated to be in the range of 15.5–17.1 kJ/mol by using the Clausius-Clapeyron equation (Fig. S9 in Supporting information) [30], which demonstrates moderate interaction between the MOF framework and guest CO_2 molecules. These findings indicate that BUT-75 would be a nice CO_2 adsorbent, favoring its application in CO_2 capture and conversion with a good affinity toward CO_2.

Considering good chemical stability, high-density exposed Co(II) sites, and selective CO_2 sorption at room temperature, the catalytic activity of BUT-75 toward the CO_2 cycloaddition with epoxides was investigated under solvent-free conditions [31–33]. Various reaction parameters (time, temperature, and catalyst dosage) were altered in the model reaction by using propylene oxide as the substrate, and the results are summarized in Table 1. BUT-75 catalyzed this reaction with a 30.1% conversion of propylene oxide in 24 h (Table 1, entry 1). After adding the phase transfer catalyst tetra-n-tertbutylammonium bromide (TBAB), BUT-75 gave a significantly higher propylene oxide conversion of 80.5% (Table1, entry 2). It could be reasoned that the presence of

Table 1
Cycloaddition of CO_2 and propylene oxide under different conditions.[a]

Entry	Catalyst	Catalyst (mg)	Temperature (°C)	Time (h)	Conversion[b] (%)	TOF[c] (h^{-1})
1	BUT-75	20	25	24	30.1	4.1
2	BUT-75/TBAB	20	25	24	80.5	11.1
3	None	â	25	24	0	0
4	TBAB	â	25	24	12.5	â
5	BUT-75/TBAB	20	25	6	12.1	6.7
6	BUT-75/TBAB	20	25	12	36.5	10.1
7	BUT-75/TBAB	20	25	48	83.2	9.2
8	BUT-75/TBAB	20	0	24	17.7	2.4
9	BUT-75/TBAB	20	50	24	93.5	12.9
10	BUT-75/TBAB	10	25	24	32.2	8.9
11	BUT-75/TBAB	30	25	24	89.3	8.3
12	BUT-75/TBAB	40	25	24	91.2	6.3

[a] Reaction conditions: propylene oxide, 20 mmol; TBAB, 0.5 mmol; with a CO_2 balloon.
[b] Conversion of propylene oxide was determined from the ^1H NMR spectra of the liquid mixture after reaction.
[c] Turnover frequency (product (mol)/ metal (mol)/time (h)).

TBAB facilitates the contact of reactants and catalysts on phase interfaces (gas to liquid and liquid to solid), thereby improving the catalysis performance of BUT-75 [34–36]. Control experiments demonstrated that no conversion of propylene oxide was observed in the absence of BUT-75 and TBAB (Table 1, entry 3), and only a conversion of 12.5% was available by using the TBAB alone (Table 1, entry 4). As a result, BUT-75 can catalyze the CO_2 cycloaddition with epoxides effectively with the assistance of TBAB. As shown in entries 2 and 5–7, the reaction had a slow reaction rate within the first 6 h, and the conversion reached 80.5% for 24 h, indicating an induction period required in the reaction. Further prolonging the reaction time cannot obviously increase the conversion of propylene oxide, 24 h is thus the optimum time for the reaction. The conversion of epoxide also increased with temperature (Table 1, entry 2, 8 and 9, from 17.7% at 0 °C to 93.5% at 50 °C) and catalyst dosage (Table 1, entry 2, 10–12, from 32.2% with 10 mg to 91.2% with 40 mg). By rationally balancing the cost and catalysis performance, the reaction catalyzed by BUT-75 of 20 mg in the presence of TBAB at 25 °C for 24 h was established as the optimal conditions.

With the optimized conditions in hand, we further expanded the substrate scope of the CO_2-epoxides cycloaddition reaction catalyzed by BUT-75. Different epoxides with various substituent groups were checked. These reactions were carried out with BUT-75 under the standard conditions. As shown in Table S2 (Supporting information), the conversions of 1,2-butene oxide, epichlorohydrin, and styrene oxide to the corresponding cyclic carbonates after 24 h are 34.1%, 27.6% and 14.8%, respectively. It can be seen that the conversions of epoxides with larger substituent groups are all lower than that of the propylene oxide with a methyl substitution (80.5%) after 24 h. When the reaction time was extended to 48 h, the obtained conversions were raised to 71.5%, 63.3% and 20.4%, still being lower than that of the propylene oxide (83.2%). These lower conversions may be attributed to that the small pore aperture of BUT-75 limits the diffusion of bulky substrates in the channel, giving rise to reduced production of the resulting cyclic carbonates [37,38].

The recyclability is also significant for a heterogeneous catalyst. The cycling experiment was conducted under standard conditions. After the reaction, the BUT-75 catalyst was separated from the system, washed, and dried for the next cycle. As shown in Fig. S10 (Supporting information), the catalytic activity of BUT-75 remains almost unchanged after five cycles. Furthermore, the FT-IR spectra, PXRD patterns, and N_2 adsorption isotherms (Figs. S4 and S11 in Supporting information) of the re-collected BUT-75 samples exhibit no obvious changes compared to those of the sample used in the first cycle, indicating its structural integrity in recycling.

Overall, the above results verify the good performance of the recyclable BUT-75 MOF as an efficient heterogeneous catalyst toward the CO_2-epoxide cycloaddition. More importantly, this conversion can proceed under ambient conditions in the presence of the BUT-75 catalyst, which can reduce the energy input and meet the requirement of green chemistry. To the best of our knowledge, only a few MOFs can catalyze this reaction under ambient conditions, among which BUT-75 is superior to others with higher efficiency (Table S3 in Supporting information).

A possible reaction mechanism is then proposed on the basis of the experimental results and previous reports (Scheme S3 in Supporting information) [39,40]. The coordinately unsaturated Co(II) ions exposed in the pores of BUT-75 serve as the active Lewis acidic sites, whose interaction to the O atom of the epoxide could activate the epoxy ring [**A**]. Then the Br^- species from the TBAB attacks the less steric-hindered carbon of the epoxide, thus opening the epoxy ring to afford the intermediate [**B**]. The oxygen anion from the epoxy ring reacts with CO_2 to form an alkylcarbonate anion [**C**]. Finally, [**C**] undergoes cyclization to give the final cyclic carbonate product [**D**], with the BUT-75 catalyst recovered for the next catalysis cycle. Based on this mechanism, the practical catalytic performance of BUT-75 largely relies on the accessibility of active Co(II) sites to the substrates. Therefore, the relatively small pores of BUT-75 prevent the bulky substrates from approaching, accounting for their reduced conversions.

In summary, a stable versatile Co(II)-MOF, BUT-75, was constructed by using a newly designed dual-functional pyrazolate-carboxylate ligand H_3PCBA. This MOF possesses a (3,6)-connected network structure with the 6-connected linear Co_3 cluster. Assembled by integrating Co—O and Co—N coordination bonds into one framework, BUT-75 has good acid/base stability in a wide pH range from 3 to 12. Besides, it showed selective CO_2 adsorption capacity over N_2 at 298 K. Due to high framework robustness and abundant open Co(II) sites, BUT-75 demonstrated good catalytic performance in the CO_2 cycloaddition reaction under ambient conditions, being a potential heterogeneous catalyst with good regeneration ability. This work opens a new door for building stable multifunctional MOFs through the rational ligand design, and thus expands their applications in addressing urgent environmental issues, such as the CO_2 fixation.

Declaration of competing interest

The authors declare that they have no known competing financial interests or personal relationships that could have appeared to influence the work reported in this paper.

Acknowledgments

This work was financially supported by the National Natural Science Foundation of China (Nos. 21771012, 21601008, 51621003) and the Science & Technology Project of Beijing Municipal Education Committee (No. KZ201810005004).

Appendix A. Supplementary data

Supplementary material related to this article can be found, in the online version, at doi:https://doi.org/10.1016/j.cclet.2020.07.023.

References

[1] J.R. Li, J. Sculley, H.C. Zhou, Chem. Rev. 112 (2012) 869–932.
[2] P. Ramaswamy, N.E. Wong, G.K.H. Shimizu, Chem. Soc. Rev. 43 (2014) 5913–5932.
[3] P. Horcajada, R. Gref, T. Baati, et al., Chem. Rev. 112 (2012) 1232–1268.
[4] L.E. Kreno, K. Leong, O.K. Farha, et al., Chem. Rev. 112 (2012) 1105–1125.
[5] L. Chen, Q. Xu, Matter 1 (2019) 57–89.
[6] B. Wang, H. Yang, Y.B. Xie, et al., Chin. Chem. Lett. 27 (2016) 502–506.
[7] T. He, Y.Z. Zhang, X.J. Kong, et al., Cryst. Growth Des. 19 (2019) 430–436.
[8] J. Li, Y. Wang, Y. Yu, Q.L. Chin, Chem. Lett. 29 (2018) 837–841.
[9] R.G. Pearson, J. Am. Chem. Soc. 85 (1963) 3533–3539.
[10] F. Yang, G. Xu, Y.B. Dou, et al., Nat. Energy 2 (2017) 877–883.
[11] X.L. Lv, S. Yuan, L.H. Xie, et al., J. Am. Chem. Soc. 141 (2019) 10283–10293.
[12] K. Wang, X.L. Lv, D. Feng, et al., J. Am. Chem. Soc. 138 (2016) 914–919.
[13] X.L. Lv, K. Wang, B. Wang, et al., J. Am. Chem. Soc. 139 (2017) 211–217.
[14] Y.L. Hu, M.L. Ding, X.Q. Liu, L.B. Sun, H.L. Jiang, Chem. Commun. 52 (2016) 5734–5737.
[15] H. He, Q.Q. Zhu, C.P. Li, M. Du, Cryst. Growth Des. 19 (2019) 694–703.
[16] N.C. Burtch, H. Jasuja, K.S. Walton, Chem. Rev. 114 (2014) 10575–10612.
[17] T. Devic, C. Serre, Chem. Soc. Rev. 43 (2014) 6097–6115.
[18] X.M. Kang, H.S. Hu, Z.L. Wu, et al., Angew. Chem. Int. Ed. 58 (2019) 16610–16616.
[19] C. Heering, I. Boldog, V. Vasylyeva, J. Sanchiz, C. Janiak, CrystEngComm 15 (2013) 9757–9768.
[20] N.M. Padial, E.Q. Procopio, C. Montoro, et al., Angew. Chem. Int. Ed. 52 (2013) 8290–8294.
[21] W.Y. Gao, R. Cai, T. Pham, et al., Chem. Mater. 27 (2015) 2144–2151.
[22] Z.J. Chen, Z. Thiam, A. Shkurenko, et al., J. Am. Chem. Soc. 141 (2019) 20480–20489.
[23] W.H. Jiang, J.L. Liu, L.Z. Niu, et al., Polyhedron 124 (2017) 191–199.
[24] S. Jin, D. Wang, J. Coord. Chem. 64 (2011) 1940–1952.

[25] H.H. Wang, L.N. Jia, L. Hou, et al., Inorg. Chem. 54 (2015) 1841–1846.
[26] A. Spek, J. Appl. Crystallogr. 36 (2003) 7–13.
[27] C.S. Cao, Z.J. Song, H. Xu, et al., Angew. Chem. Int. Ed. 59 (2020) 8586–8593.
[28] O. Alduhaish, B. Li, H. Arman, et al., Chin. Chem. Lett. 28 (2017) 1653–1658.
[29] J. An, S.J. Geib, N.L. Rosi, J. Am. Chem. Soc. 132 (2010) 38–39.
[30] M. Dincă, J.R. Long, J. Am. Chem. Soc. 127 (2005) 9376–9377.
[31] J. Liang, Y.B. Huang, R. Cao, Coord. Chem. Rev. 378 (2019) 32–65.
[32] G. Xiong, B. Yu, J. Dong, et al., Chem. Commun. 53 (2017) 6013–6016.
[33] L. Zhang, S. Yuan, L. Feng, et al., Angew. Chem. Int. Ed. 57 (2018) 5095–5099.
[34] J. Song, Z. Zhang, S. Hu, et al., Green Chem. 11 (2009) 1031–1036.
[35] Y.L. Wu, G.P. Yang, S. Cheng, et al., ACS Appl. Mater. Inter. 11 (2019) 47437–47445.
[36] M.H. Beyzavi, R.C. Klet, S. Tussupbayev, et al., J. Am. Chem. Soc. 136 (2014) 15861–15864.
[37] Y. Sun, X. Jia, H. Huang, et al., J. Mater. Chem. A 8 (2020) 3180–3185.
[38] H. Hu, D.S. Zhang, H.L. Liu, et al., Chin. Chem. Lett. 32 (2020) 557–560.
[39] H. Xu, C.S. Cao, H.S. Hu, et al., Angew. Chem. Int. Ed. 58 (2019) 6022–6027.
[40] S.L. Hou, J. Dong, B. Zhao, Adv. Mater. 32 (2020) 1806163.